



Published in final edited form as:

Pharm Res. 2015 May ; 32(5): 1663–1675. doi:10.1007/s11095-014-1565-2.

Phospho-NSAIDs have enhanced efficacy in mice lacking plasma carboxylesterase: Implications for their clinical pharmacology

Chi C. Wong^{1,2}, Ka-Wing Cheng¹, Ioannis Papayannis¹, George Mattheolabakis¹, Liqun Huang¹, Gang Xie¹, Nengtai Ouyang¹, and Basil Rigas¹

¹Division of Cancer Prevention, Department of Medicine, Stony Brook University, Stony Brook, New York, USA

²Department of Medicine and Therapeutics, Chinese University of Hong Kong, Hong Kong

Abstract

Purpose—The purpose of the study was to evaluate the metabolism, pharmacokinetics and efficacy of phospho-NSAIDs in *Ces1c*-knockout mice.

Methods—Hydrolysis of phospho-NSAIDs by *Ces1c* was investigated using *Ces1c*-overexpressing cells. The rate of phospho-NSAID hydrolysis was compared between wild-type, *Ces1c*^{+/−} and *Ces1c*^{−/−} mouse plasma *in vitro*, and the effect of plasma *Ces1c* on the cytotoxicity of phospho-NSAIDs was evaluated. Pharmacokinetics of phospho-sulindac was examined in wild-type and *Ces1c*^{−/−} mice. The impact of *Ces1c* on the efficacy of phospho-sulindac was investigated using lung and pancreatic cancer models *in vivo*.

Results—Phospho-NSAIDs were extensively hydrolyzed in *Ces1c*-overexpressing cells. Phospho-NSAID hydrolysis in wild-type mouse plasma was 6- to 530-fold higher than that in the plasma of *Ces1c*^{−/−} mice. *Ces1c*-expressing wild-type mouse serum attenuated the *in vitro* cytotoxicity of phospho-NSAIDs towards cancer cells. Pharmacokinetic studies of phospho-sulindac using wild-type and *Ces1c*^{−/−} mice demonstrated 2-fold less inactivation of phospho-sulindac in the latter. Phospho-sulindac was 2-fold more efficacious in inhibiting the growth of lung and pancreatic carcinoma in *Ces1c*^{−/−} mice, as compared to wild-type mice.

Conclusions—Our results indicate that intact phospho-NSAIDs are the pharmacologically active entities and phospho-NSAIDs are expected to be more efficacious in humans than in rodents due to their differential expression of carboxylesterases.

Keywords

Non-steroidal anti-inflammatory drugs; Carboxylesterase; Pharmacokinetics; Xenografts

Corresponding author: Basil Rigas, Division of Cancer Prevention, Stony Brook University, HSC, T-17 Room 080, Stony Brook, NY 11794-8173, USA, Tel: 631-444-9538; Fax: 631-444-9553; basil.rigas@stonybrookmedicine.edu.

Conflicts of interest

The authors have nothing to disclose except for Basil Rigas, who has an equity position in Medicon Pharmaceuticals, Inc.

Introduction

The use of non-steroidal anti-inflammatory drugs (NSAIDs) is associated with reduced risk of several types of cancer (1, 2). Chronic consumption of conventional NSAIDs, such as aspirin, ibuprofen, indomethacin, naproxen and sulindac, however, causes significant gastrointestinal side effects due to the non-selective inhibition of cyclooxygenase (COX)-1 (3). A newer generation of NSAIDs, such as celecoxib and rofecoxib, selectively targets COX-2 and has diminished gastrointestinal toxicity, but they unexpectedly raise the risk of stroke and myocardial infarction (4). Given the limited anticancer efficacy (< 50%) of NSAIDs, their adverse effects outweigh clinical benefits in most patients (5).

We have developed a series of novel phospho-modified NSAIDs (6–9), consisting of an NSAID attached to a diethyl-phosphate group via a linker. The benefits of such a modification are two-fold: enhanced therapeutic efficacy and improved safety. Phospho-NSAIDs have demonstrated impressive efficacy in pre-clinical models of breast (10, 11), colon (8), lung (12), pancreatic (9) and skin (13) cancers; and are much safer than the conventional NSAIDs. Phospho-sulindac (P-S), the most extensively studied example, is 12- to 15-fold more potent in inhibiting the growth of colon cancer cells than sulindac (8). Phospho-NSAIDs are thus pharmacologically more potent molecules than their parent NSAIDs.

Biochemical evidence and animal studies indicate that carboxylesterases (CES) are the major enzymes involved in the metabolic inactivation of phospho-NSAIDs. This family of enzymes play a critical role in the inactivation of xenobiotics (14, 15). Carboxylesterases hydrolyze phospho-NSAIDs at the carboxylic ester bond, leading to the release of the native NSAID and the phospho-moiety (16, 17). Cell lines engineered to overexpress CES 1 or CES 2 actively hydrolyse phospho-NSAIDs, leading to strong resistance to their cytotoxic effects (16). In rodents, carboxylesterase-mediated inactivation of phospho-NSAIDs occurs very rapidly, resulting in very low concentrations of the intact drug in the plasma and organs (17, 18). Importantly, there are considerable differences in the expression of carboxylesterases between humans and rodents. Human plasma has no detectable carboxylesterases (19). In contrast, mouse plasma contains the plasma carboxylesterase (ES1; *Ces1c*), which contributes to a very high carboxylesterase activity. Hence, the prediction of tumor responses to phospho-NSAIDs in humans based on murine efficacy data may lead to underestimation of anticancer efficacy, due to increased inactivation of these drugs in the mouse plasma.

Recently, a *Ces1c*-knockout mouse model has been described (20). Homozygous *Ces1c* $-/-$ mice have no detectable carboxylesterase activity in the plasma, but they retain normal carboxylesterase activity in tissues. Mice possess a much richer repertoire of carboxylesterase enzymes, and it is possible other isoforms are also present in the plasma. Whilst the carboxylesterase activity of *Ces1c* $-/-$ mice is not exactly identical to that of the human plasma, it is a much more realistic model as compared to WT mice, which possess esterase activity up to hundreds of fold higher than that in humans. Homozygous *Ces1c* $-/-$ mice are therefore a reasonable model for the preclinical efficacy evaluation of phospho-NSAIDs and other ester-containing anticancer drugs, such as irinotecan and capecitabine.

We hypothesized that the rodent plasma is very efficient in phospho-NSAID hydrolysis; phospho-NSAIDs would be more efficacious in *Ces1c* $-/-$ mice due to improved metabolic stability of these drugs; and the *Ces1c* $-/-$ mice provide a more accurate reflection of the metabolism and efficacy of phospho-NSAIDs in humans.

Herein, we establish that phospho-NSAIDs undergo rapid hydrolysis in the rodent plasma that is in stark contrast to their high stability in human plasma. The rapid metabolic inactivation in turn results in a significant reduction of their anticancer effects in rodent models of human cancers. Given the significant impact of *Ces1c* on phospho-NSAID inactivation, and the discordance of carboxylesterase activity between humans and rodents, we performed pharmacokinetic and efficacy studies in wild-type and *Ces1c* $-/-$ mice to assess the impact of plasma carboxylesterase on the anticancer activity of these drugs *in vivo*.

Materials and Methods

Reagents

Phospho-sulindac (P-S, OXT-328), phospho-aspirin (MDC-46, MDC-22), phospho-ibuprofen (MDC-917), phospho-naproxen, phospho-indomethacin and phospho-tyrosol-indomethacin were gifts from Medicon Pharmaceuticals, Inc, Stony Brook, NY. Murine carboxylesterase 1C (*Ces1c*; Genbank accession number BC028907) plasmid was obtained from Open Biosystems (Huntsville, AL). Lipofectamine 2000 was purchased from Life technologies (Carlsbad, CA). All other chemicals, unless otherwise stated, were purchased from Sigma-Aldrich (St Louis, MO).

Cell culture

293T and Lewis lung carcinoma (LLC) cells were purchased from the American Type Culture Collection (ATCC, Manassas, VA). FC1245 (KPC, murine pancreatic cancer) was a gift from Dr. David Tuveson (Cold Spring Harbour Laboratory). The three cell lines were cultured in DMEM media supplemented with 10% fetal bovine serum and 50U/ml penicillin-streptomycin (Cellgro). All experiments were performed with cells between passages 1 to 10. For transfection experiments, 293T cells were seeded in 6-well plates (1×10^6 cells per well) one day prior to transfection. 293T cells were transfected with *Ces1c*-expressing plasmid, or the empty vector with Lipofectamine 2000 according to manufacturer's instructions. Over-expression of *Ces1c* was confirmed by quantitative RT-PCR and by the hydrolysis of model substrate *p*-nitrophenyl acetate. Antibiotics were not added for the transfection experiments.

Enzyme preparation and *In vitro* carboxylesterase activity assay

293T cells transfected with *Ces1c* plasmid or empty vector were harvested in PBS 48 h post-transfection and homogenized by sonication. Cellular extracts were stored at -80 °C without the addition of protease inhibitors. For *in vitro* assay, cell extracts (2–10 μ L) from the empty vector and *Ces1c* expressing cells were respectively diluted with pre-warmed 100 mM phosphate buffer (pH 7.4) at 37 °C in a total volume of 100 μ L. The reaction was then initiated by the addition of phospho-NSAIDs. At the end of the incubation period, the

reaction was stopped by the addition of 400 μ L ice-cold acetonitrile. After centrifugation at 15,000 g for 15 min, the supernatant was analyzed by HPLC. Apparent enzyme kinetic parameters were estimated in terms of product formation, using various concentrations of substrates.

Growth inhibition assays

LLC (1×10^4 cells per well), KPC (1×10^4 cells per well) or 293T (3.5×10^4 cells per well) cells were seeded in 96-well plates. After overnight incubation, various concentrations of phospho-NSAIDs were added, after which the cells were incubated for 24 h. At the end of the incubation, cell viability was determined by a modified 3-[4,5-dimethylthiazol-2-yl]-2,5-diphenyltetrazolium bromide (MTT) colorimetric assay.

Animals

Heterozygous *Ces1c* +/- mice (Stock no: 014096) on C57BL/6 background were purchased from Jackson Laboratory (Bar Harbor, ME). Heterozygous *Ces1c* +/- mice were bred to obtain *Ces1c* +/+, *Ces1c* +/- and *Ces1c* -/- knockout mice. *Ces1c* -/- mice are viable and fertile, so we also maintained a *Ces1c* -/- knockout line by breeding homozygotes. All animal studies were approved by the Institutional Animal Care and Use Committee at Stony Brook University.

Pharmacokinetics and biodistribution

Ces1c +/+, *Ces1c* +/- and *Ces1c* -/- knockout mice of ~8 to 10 weeks old were treated with a single dose of P-S (300 mg/kg in corn oil, i.p. or p.o.), P-S-loaded PLA-PEG (50 mg/kg, i.v.) or P-S-loaded Pluronic P-123 (50 mg/kg, i.v.). The mice were euthanized at designated time points and blood samples were collected by cardiac puncture. The blood samples were immediately extracted with two volumes of acetonitrile. Tissues were homogenized, sonicated and extracted with acetonitrile. The levels of P-S and its metabolites were determined by HPLC. Pharmacokinetic parameters were calculated using the PK Solver plug-in for Microsoft Excel (21). For P-S given i.p. (300 mg/kg), a one-compartment model (extravascular) with first-order absorption and elimination kinetics provided the best fitting of the plasma disappearance curve. The plasma disappearance curves for sulindac in all pharmacokinetic experiments were also fitted using the same model. For P-S given i.v., the data were fitted using a one-compartment model (i.v. bolus), which provided the best fitting of the plasma disappearance curves. Parameters derived are as follows: C_0 : drug concentration at time 0; C_{max} : peak plasma concentration; T_{max} : time to reach peak plasma concentration; AUC_{0-24h} : area under curve (0–24 h); $t_{1/2}$: elimination half-life; CL: clearance; and V_{ss} : volume of distribution at steady state.

Efficacy studies

Subcutaneous xenografts models—Male *Ces1c* +/+ and *Ces1c* -/- mice (9–10 weeks old) were inoculated subcutaneously in their left and right flanks, each with 5×10^5 LLC or KPC cells suspended in 100 μ L of phosphate-buffered saline. When the average tumor size reached ~180 mm³, *Ces1c* +/+ and *Ces1c* -/- mice were divided into groups and given respectively the following treatments: vehicle, P-S (150 mg/kg, i.p.), PLA-PEG P-S (50

mg/kg, i.v.) or Pluronic P123 P-S (50 mg/kg, i.v.). In each experiment, we randomized the mice such that the starting tumor volumes between vehicle and treatment groups were within 10 mm³. Tumor dimensions (n = 8 per group) were measured at designated time points with a digital caliper twice a week, and tumor volumes were calculated using the following formula: tumor volume = [length × width × (length + width/2) × 0.56] (6). At the end of the treatment period, the animals were sacrificed and their tumors were excised and weighed. Harvested tumors were homogenized, sonicated and extracted with acetonitrile. Tumor drug levels were determined as described above.

Orthotopic xenografts model—Male *Ces1c* *+/+* and *Ces1c* *-/-* mice (9–10 weeks old) were anaesthetized and a small incision was made in the left abdomen to expose the pancreas. 2.5×10^5 KPC cells suspended in 50 μ L of phosphate-buffered saline were injected into the pancreas with a 28G insulin needle. After surgery, the mice were randomized into vehicle and P-V (30 mg/kg/d, i.p.) treatment groups. At the end of the treatment period, the animals were sacrificed and their pancreas (cancerous and non-cancerous tissues) were excised and weighed.

HPLC analysis

HPLC was used to analyze the levels of phospho-NSAIDs and their hydrolyzed products in *in vitro* incubations, and in the plasma and tissues. The HPLC system consisted of a Waters Alliance 2695 Separations Module equipped with a Waters 2998 photo-diode array detector (220 nm) (Waters, Milford, MA) and a Thermo BDS Hypersil C18 column (150 × 4.6 mm, particle size 3 μ m) (Thermo Fisher Scientific, Waltham, MA). The mobile phase consisted of a gradient between buffer A (formic acid, acetonitrile, H₂O (0.1:4.9:95, v/v/v)) and 100 % acetonitrile.

Data analysis

Data are shown as mean \pm SEM. Raw data from the kinetic studies and cell growth assays were analyzed using GraphPad Prism 5 (Graphpad Software, San Diego, CA). K_m and V_{max} were derived from a nonlinear regression fit of the Michaelis–Menten model. Statistical differences were determined using analysis of variance using the Student's *t*-test (two-sided). Differences were considered significant when $p < 0.05$.

Results

Phospho-NSAID hydrolysis by murine plasma carboxylesterase

To evaluate the hydrolysis of phospho-NSAIDs by murine plasma carboxylesterase (Figure 1), kinetic studies were performed with cell lysates from *Ces1c*-overexpressing human embryonic kidney 293T cells to determine the parameters K_m and V_{max} . The kinetic parameters are shown in Table 1. With the exception of the phospho-aspirin derivatives (MDC-46 and MDC-22), phospho-NSAIDs exhibited a moderate affinity ($K_m < 100 \mu$ M) towards *Ces1c*, with phospho-tyrosol-indomethacin and phospho-indomethacin having the lowest K_m values. We observed that the K_m values of phospho-NSAIDs towards *Ces1c* decreased with increasing hydrophobicity, although this association did not reach statistical significance ($p=0.056$). The highest V_{max} values were observed with phospho-tyrosol-

indomethacin, followed by phospho-naproxen. Catalytic efficiency (V_{\max}/K_m) of Ces1c was in the following order: phospho-tyrosol-indomethacin > phospho-indomethacin > phospho-ibuprofen > phospho-naproxen > P-S > MDC-46 > MDC-22. Our results indicate that the murine plasma carboxylesterase (Ces1c) is capable of catalysing the hydrolysis of all phospho-NSAIDs examined.

Phospho-NSAID inactivation by wild-type, Ces1c +/- and Ces1c -/- mouse plasma and tissues

To assess the effect of plasma Ces1c knockout on the metabolism of phospho-NSAIDs, we incubated phospho-NSAIDs (100 μ M) with wild-type, Ces1c +/- and Ces1c -/- mouse plasma respectively and identified the resulting metabolites by HPLC. As shown in Table 2, wild-type mouse plasma possessed the highest hydrolytic activity for all phospho-NSAIDs evaluated; Ces1c +/- mice had intermediate hydrolytic activity; while Ces1c -/- had the lowest hydrolytic activity. This is in concordance with our hypothesis that Ces1c contributes significantly to the metabolism of phospho-NSAIDs in mouse plasma.

As shown in Table 2, the most striking difference was found for P-S. The rate of hydrolysis of P-S in wild type and Ces1c -/- plasma was 1.06 ± 0.05 and 0.01 ± 0.00 nmol/min/mg, respectively, which represents a 106-fold difference. Wild-type mouse plasma also hydrolysed all the other phospho-NSAIDs 5- to 22-fold more rapidly than Ces1c -/- mouse plasma. The fold differences between wild type and Ces1c -/- plasma for other drugs are as follows: phospho-naproxen = 12; phospho-tyrosol-indomethacin = 7; phospho-indomethacin = 22; phospho-ibuprofen = 5; and MDC-46 = 6. These data suggest that Ces1c contributes 80 to >99% of the carboxylesterase activity towards phospho-NSAIDs in the wild-type mouse plasma. An exception was phospho-aspirin (MDC-22), which was rapidly hydrolyzed in Ces1c -/- mouse plasma as well as in wild-type plasma. Ces1c -/- mouse plasma also appeared to retain a low but detectable residual esterase activity for other phospho-NSAIDs, which indicates the potential existence of other esterase(s) in mouse plasma that can metabolize these drugs.

We also evaluated the hydrolytic activity of human plasma for phospho-NSAIDs (Table 2). Consistent with its lack of carboxylesterase expression (19), it exhibited minimal hydrolytic activities towards phospho-NSAIDs that were 6- to 530-fold lower than those of wild-type mouse plasma. Importantly, esterase activity of the Ces1c -/- plasma (0.5 to 5-fold compared to the human plasma) closely reflects the hydrolytic activity of the human plasma, with the exception of phospho-aspirin (MDC-22). Hence, Ces1c -/- mice may represent a more accurate model of human metabolism of phospho-NSAIDs.

To determine whether Ces1c knockout also affects the hydrolytic activity in Ces1c -/- mouse tissues, we evaluated the hydrolysis of P-S by tissue extracts from wild-type, Ces1c +/- and Ces1c -/- mice (Figure 1). All the tissues from Ces1c -/- mice, except the small intestine and the spleen, showed a comparable hydrolytic activity towards P-S compared to the corresponding tissues from wild-type mice. Of note, the hydrolytic activity of wild-type plasma towards P-S was higher than that of all organs/tissues evaluated. Deletion of Ces1c gene (expressed specifically in blood) therefore selectively abrogates carboxylesterase activity in the mouse plasma, which is capable of rapid hydrolysis of phospho-NSAIDs.

Cytotoxic activity of phospho-NSAIDs is attenuated in the presence of murine plasma carboxylesterase

We have reported previously that phospho-NSAIDs inhibited the growth of cancer cells more potently compared to their parent NSAIDs. Consequently, the hydrolysis of phospho-NSAIDs by carboxylesterases may lead to their inactivation, resulting in reduced efficacy (16). We over-expressed Ces1c in 293T cells and determined the 24-h IC₅₀ values of phospho-NSAIDs. In control vector-transfected cells, phospho-NSAIDs were highly cytotoxic with IC₅₀ values of < 70 μM (16). Phospho-aspirins (MDC-46 and MDC-22) were the exceptions, with IC₅₀ values of 953 and 507 μM, respectively (Table 3). Expression of Ces1c resulted in higher IC₅₀ values for most of the phospho-NSAIDs. In particular, the IC₅₀ values for phospho-ibuprofen and phospho-naproxen were dramatically increased by 13- and 19-fold, respectively. Ces1c expression also considerably reduced the cytotoxicity of phospho-tyrosol-indomethacin (5.0-fold), P-S (4.0-fold), phospho-valproic acid (2.6-fold) and phospho-indomethacin (2.3-fold). The rate of hydrolysis may be a key factor in determining the relative IC₅₀ values in control and Ces1c-expressing cells, since phospho-NSAIDs with the highest rate of hydrolysis, such as phospho-ibuprofen, phospho-naproxen and phospho-tyrosol-indomethacin (Table 1) also showed the greatest fold-reduction in cytotoxicity in Ces1c-expressing cells. However, Ces1c had little impact on the cytotoxicity of phospho-aspirins (MDC-46 and MDC-22), despite significant hydrolytic activity of Ces1c.

We then examined the direct effect of wild-type and Ces1c *-/-* mouse serum on the cytotoxicity of phospho-NSAIDs in cancer cell lines (Table 4). When cultured in the presence of FBS whose enzymatic activity had been heat inactivated, LLC (IC₅₀: 68 to 266 μM) and KPC (IC₅₀: 29 to 498 μM) cells were sensitive to the cytotoxic effects of phospho-NSAIDs, except phospho-aspirins (MDC-46 and MDC22) that were weakly cytotoxic (IC₅₀ values >750 μM, data not shown). Addition of 5% wild-type mouse serum significantly attenuated the cytotoxicity of phospho-NSAIDs in these cancer cell lines. Overall, their 24-h IC₅₀ values were increased by 6–30-fold in LLC cells (395 to 2,000 μM) and 4–68-fold in KPC cells (513 to >2,000 μM). Wild-type serum had a particularly dramatic effect on the cytotoxicity of phospho-ibuprofen, phospho-valproic acid and phospho-indomethacin. On the other hand, the presence of 5% Ces1c *-/-* mouse serum had little impact (1–2-fold) on the cytotoxicity of phospho-NSAIDs in LLC (61–441 μM) and KPC (76–780 μM) cells. Our results indicate that murine plasma carboxylesterase (Ces1c) in the wild-type mice is capable of rapid attenuation of the anticancer activity of phospho-NSAIDs. Given that carboxylesterases are absent in the human plasma, our data provide the rationale for the use of Ces1c *-/-* mice for the pharmacokinetic and efficacy evaluation of these compounds.

Pharmacokinetics of P-S in wild-type and Ces1c *-/-* mice

Having shown that the murine plasma carboxylesterase plays a major role in the metabolic inactivation and cytotoxic activity of phospho-NSAIDs *in vitro*, we next compared the pharmacokinetic profiles and tissue distribution of P-S in wild-type and Ces1c *-/-* mice *in vivo*, using different routes (i.p. and i.v.) of administration.

Pharmacokinetic properties of P-S were evaluated in wild-type and *Ces1c* $-/-$ mice after a single i.p. injection (300 mg/kg) (Figure 2A and Table 5). A significantly higher peak level (at 0.5 h) of intact P-S was detected in *Ces1c* $-/-$ mice (77 μ M) compared to that in wild-type mice (40 μ M); and the 24-h total drug exposure (AUC_{0-24h}) was 1.7-fold higher in the former (261 vs. 155 μ Mxh). In contrast, the peak levels (C_{max}) and AUC_{0-24h} of hydrolyzed P-S metabolites (sulindac, sulindac sulfone, and sulindac sulfide) were lower in *Ces1c* $-/-$ mice compared to those in wild-type mice (Supplementary Table 1–3). Therefore, the bioavailability of P-S administered i.p. is enhanced in *Ces1c* $-/-$ mice, an effect which could be attributed to reduced hydrolysis in the absence of plasma *Ces1c*.

P-S is poorly soluble in water, thus necessitating the use of a carrier for its i.v. administration. We have incorporated P-S into two nano-carrier formulations, Pluronic P123 and PLA-PEG. *In vitro* analysis showed that Pluronic P123 micelles primarily function to assist solubilization of P-S in the aqueous milieu without significant protection from carboxylesterases; PLA-PEG nanoparticles confer resistance to carboxylesterase-mediated hydrolysis. Next, we evaluated the pharmacokinetics of P-S in these two formulations in wild-type and *Ces1c* $-/-$ mice after a single i.v. injection.

As shown in Figure 2B, intact P-S was detected in both the blood of the wild-type and *Ces1c* $-/-$ mice following a single dose of Pluronic P123 P-S (50 mg/kg). Blood levels of intact P-S peaked at the first time point (5 min). A higher level of intact P-S was detected in *Ces1c* $-/-$ mice (32 μ M) compared to wild-type mice (19 μ M) and their concentrations decreased rapidly thereafter; and the AUC_{0-24h} was increased by 2.8-fold in *Ces1c* $-/-$ mice (11 versus 4 μ M*h). We observed higher levels of intact P-S following administration of PLA-PEG P-S (50 mg/kg), presumably due to the enhanced protection and circulation time of PLA-PEG nanoparticles (Figure 2C). The levels of intact PS were similar between *Ces1c* $-/-$ and wild-type mice after 5 min. However, at later time points (15 min to 24 h) higher levels of intact PS were observed in *Ces1c* $-/-$ mice; and the AUC_{0-24h} was 2.1-fold higher than that in wild-type mice.

Corresponding to the higher levels of intact P-S, the levels (AUC_{0-24h}) of P-S metabolites were lower in *Ces1c* $-/-$ mice compared to those in wild-type mice for both Pluronic P123 and PLA-PEG-incorporated P-S. Our results indicate that plasma *Ces1c* plays an important role in the metabolic inactivation of P-S; and that *Ces1c* knockout improves the pharmacokinetic properties of P-S following i.v. administration independently of the nature of the nano-carrier formulation(s) employed.

Biodistribution of P-S in wild-type and *Ces1c* $-/-$ mice

To evaluate the effect of *Ces1c* expression on the biodistribution of P-S in mice, we assessed the drug levels in six major organs (heart, kidney, liver, lung, small intestine and spleen) following i.v. administration (Figure 3A & B).

After a single i.v. administration with Pluronic P123 P-S, the highest levels of intact P-S were found in the liver, and were essentially the same in both wild type and *Ces1c* $-/-$ mice (~130 nmol/mg protein). In extra-hepatic organs, intact P-S was preferentially distributed to the lungs, the heart and the kidneys. Notably, the levels of intact P-S in these organs were

much higher (3.7- to 7.6-fold) in *Ces1c* $-/-$ mice than those in wild-type mice. Biodistribution of intact P-S was similarly enhanced in *Ces1c* $-/-$ mice after i.v. treatment with PLA-PEG P-S. In extra-hepatic organs, the levels of intact P-S were 1.7- to 2-fold higher in *Ces1c* $-/-$ mice compared to those in wild-type mice; while the levels of intact P-S in the liver were similar. The highest levels of P-S were detected in the lungs (~600 nmol/mg protein in *Ces1c* $-/-$ mice), suggesting that the encapsulation of P-S in PLA-PEG altered its biodistribution *in vivo*. The levels of P-S metabolites followed a reverse trend; their tissue levels were generally higher in the wild-type mice than in *Ces1c* $-/-$ mice. In other words, these results show that when P-S is exposed to blood CES, it is hydrolysed, resulting in higher tissue levels of its hydrolytic product, sulindac. In contrast, when P-S is protected from CES by its formulation, the tissue levels of sulindac are similar between wild-type and *Ces1c* $-/-$ mice.

Our data suggest that plasma *Ces1c* has a critical impact on the biodistribution of P-S. The striking improvement in the biodistribution of P-S in the absence of *Ces1c* has important implications for its efficacy *in vivo*, given that P-S possesses much more potent anticancer activity compared to any of its metabolites.

Efficacy of P-S in wild-type and *Ces1c* $-/-$ mice bearing LLC xenografts

Given that *Ces1c* knockout significantly improved the pharmacokinetics and biodistribution of intact P-S, we investigated the pharmacological relevance of *Ces1c* knockout by comparing the efficacy of phospho-modified drugs in wild-type and *Ces1c* $-/-$ mice bearing subcutaneous lung cancer xenografts.

First, we evaluated the efficacy of P-S (150 mg/kg/d, i.p.) in wild-type and *Ces1c* $-/-$ mice bearing s.c. LLC xenografts. PS is known to be efficacious in murine models of human lung cancer (12). As shown in Figure 4A and 4C, P-S suppressed tumor growth more potently in *Ces1c* $-/-$ mice than in wild-type mice. The growth inhibitory effect of P-S in the *Ces1c* $-/-$ mice was statistically significant beginning 3 days after the initiation of treatment until the end of the study ($p=0.03-0.04$, compared to *Ces1c* $-/-$ vehicle); whereas P-S in the wild-type only moderately (and statistically not significant; $p>0.05$, compared to wild-type vehicle) inhibited tumor growth at all the time points. At the end of the study (day 9), P-S inhibited tumor growth in the *Ces1c* $-/-$ mice by 81%; and by 41% in the wild-type mice relative to the controls. P-S also reduced tumor weight by 74% ($p=0.002$ compared to *Ces1c* $-/-$ vehicle) and 35% ($p=0.1$, compared to wild type vehicle) in the *Ces1c* $-/-$ and the wild-type mice, respectively (Suppl. Figure 1).

Next, we evaluated the impact of *Ces1c* knockout on the efficacy of P-S given intravenously (Figure 4B). P-S was encapsulated in Pluronic P123 (50 mg/kg) and PLA-PEG (50 mg/kg), respectively. In both the wild-type and *Ces1c* $-/-$ mice, Pluronic P123 and PLA-PEG P-S significantly inhibited tumor growth starting on day 5 after the start of treatment until the end of the study ($p<0.04$ compared to their respective vehicle groups). Moreover, the efficacy of P-S in either formulation was stronger in the *Ces1c* $-/-$ mice (64–73% inhibition) compared to that in the wild-type mice (28–39% inhibition). Reduction in tumor weight by P-S was also higher in the *Ces1c* $-/-$ mice (63–73%) than in the wild-type mice

(29%). Hence, P-S given via i.p. or i.v. showed superior efficacy in the *Ces1c* $-/-$ compared to the wild-type mice.

To determine whether the superior efficacy of P-S in *Ces1c* $-/-$ mice is a result of the improved pharmacokinetics and biodistribution of the intact drug, we compared the endpoint levels of P-S and its metabolites in the plasma and tumors from mice treated with P-S (i.p.), Pluronic P123 P-S and PLA-PEG P-S, respectively. Consistent with the pharmacokinetic studies, blood levels of intact P-S were 1.5-fold higher in *Ces1c* $-/-$ mice compared to those in wild-type mice. Remarkably, the levels of intact P-S in tumors were over 3-fold higher in *Ces1c* $-/-$ mice than those in wild-type mice, irrespective of the route of delivery (Figure 4D and 4E). Corresponding to the reduced P-S hydrolysis, the levels of sulindac in LLC xenografts were lower in the *Ces1c* $-/-$ than those in the wild-type mice.

Of interest, intact P-S levels in tumors were positively correlated with the therapeutic efficacy (% inhibition by volume) in LLC xenografts ($R=0.84$, $p<0.05$). However, no such correlation was observed between efficacy and tumor levels of sulindac, sulindac sulfone or sulindac sulfide. These findings suggest that the absence of carboxylesterase improves the delivery of intact P-S to tumors, leading to enhanced efficacy *in vivo*.

Efficacy of P-S and P-V in wild-type and *Ces1c* $-/-$ mice bearing pancreatic carcinomas

To rule out a cell-line specific effect, we investigated the effect of *Ces1c* knockout on the efficacy of P-S in murine pancreatic carcinoma. Wild-type and *Ces1c* $-/-$ mice bearing s.c. FC1245 xenografts were treated with P-S (150/mg/kg/d, i.p.). In agreement with the results from the LLC xenograft study, P-S was significantly more effective in inhibiting the growth of FC1245 xenografts in the *Ces1c* $-/-$ mice (50% inhibition, $p<0.05$) than in the wild-type mice (23% inhibition) (Figure 5A).

Since plasma carboxylesterase is capable of inactivating a broad range of phospho-modified drugs, we further evaluated the efficacy of P-V, an inhibitor of pancreatic cancer which targets STAT3 (22), in s.c. and orthotopic FC1245 xenografts. P-V suppressed the growth of s.c. FC1245 xenografts more potently in *Ces1c* $-/-$ than in wild-type mice (Figure 5B). We then evaluated the efficacy of P-V in an orthotopic model of pancreatic cancer, and also observed a therapeutic advantage in *Ces1c* $-/-$ mice (Figure 5C). Thus, knockout of *Ces1c* appears to also improve the efficacy of P-V, another prototypical phospho-modified drug.

Discussion

Our data established that a) murine plasma carboxylesterase (*Ces1c*, ES-1) mediates the hydrolysis of phospho-NSAIDs *in vitro* and *in vivo*; b) *Ces1c* rapidly inactivates phospho-NSAIDs, resulting in a reduction in their anticancer activity; and c) knockout of *Ces1c* in mice improves the pharmacokinetics and biodistribution of phospho-NSAIDs, leading to an enhanced anticancer efficacy *in vivo*. Given the impact of murine *Ces1c* on the pharmacological activity of phospho-NSAIDs and that the human plasma does not have carboxylesterase activity, our findings provide a biological rationale for the use of *Ces1c* knockout mice for the pharmacokinetic and efficacy evaluation of this class of anticancer agents, as these mice may represent a more accurate model of human drug metabolism.

Phospho-NSAIDs are a novel class of anticancer drugs that have demonstrated strong inhibitory effects in preclinical models of human cancers (6,13,16, 23). A common structural feature of these phospho-modified drugs is the presence of a carboxylic ester bond linking the parent NSAIDs to a phospho-head group via a linker; and the integrity of this linkage is critical for the pharmacological activity of the drugs. Previous investigations have shown that human carboxylesterases, such as CES1 (liver isoform) and CES2 (intestinal isoform), play a key role in the hydrolysis and subsequent inactivation of phospho-NSAIDs (16). Apart from the liver and intestinal carboxylesterases, mice additionally express Ces1c in the plasma, which may further contribute to the accelerated inactivation of phospho-NSAIDs *in vivo*. Indeed, we have demonstrated that Ces1c over-expressed in human cells mediates phospho-NSAIDs hydrolysis and that the wild-type mouse plasma hydrolyzes phospho-NSAIDs 6- to 530-fold more rapidly than the human plasma. Importantly, wild-type mouse plasma catalyzes P-S hydrolysis most efficiently among all tissues evaluated, suggesting that the plasma may play a dominant role in its hydrolytic inactivation in mice. Accordingly, we observed strong attenuation of the anticancer activity of phospho-NSAIDs *in vitro* upon either ectopic over-expression of Ces1c, or in the presence of wild-type mouse plasma. Since human plasma is much less efficient in phospho-NSAID metabolism compared to mouse plasma, it makes the extrapolation of antitumor and pharmacokinetic properties using wild-type mice difficult.

To mimic the human metabolism of phospho-NSAIDs, we employed a Ces1c knockout mouse model to evaluate their pharmacokinetics and efficacy *in vivo*. Esterase-mediated hydrolysis of phospho-NSAIDs in Ces1c $-/-$ mouse plasma was strongly attenuated compared to that in wild-type plasma, and as such closely reflects the human plasma. As a result, Ces1c $-/-$ mouse plasma has a limited impact on the cytotoxicity of phospho-NSAIDs *in vitro*. Comparative pharmacokinetic and biodistribution studies using P-S as a prototypical phospho-NSAID in the wild-type and Ces1c $-/-$ mice revealed that the knockout of Ces1c in mouse plasma contributes to an improved delivery of the intact drug, irrespective of the route of administration and drug formulation utilized. Hence, the presence of Ces1c constitutes a major barrier to the delivery of the intact phospho-NSAIDs to the target site(s) *in vivo*.

The enhanced delivery of intact P-S in Ces1c $-/-$ mice is highly consequential, as the efficacy of P-S, given either i.p. or i.v., in the treatment of lung and pancreatic carcinomas was improved by nearly 2-fold in Ces1c $-/-$ mice as compared to that in wild-type mice. Consistent with the improved biodistribution of P-S in Ces1c $-/-$ mice, we observed >3-fold higher levels of intact P-S in the tumors in these mice. Notably, there was a significant positive correlation between the levels of intact P-S, but not its hydrolyzed metabolites, and therapeutic efficacy. These results suggest that intact P-S is the pharmacologically active entity. This observation is reinforced by the increased efficacy of phospho-valproic acid, another phospho-modified drug, in Ces1c $-/-$ mice bearing pancreatic carcinomas. Given that all of our previous studies were performed exclusively on wild-type mice, it is reasonable to assume that the anticancer efficacy of phospho-NSAIDs would be even more impressive in Ces1c $-/-$ mice as well as in humans, both of which lacking in plasma esterase activity. While Ces1c knockout improves the delivery of intact P-S, it does not

eliminate the hydrolysis of P-S due to the carboxylesterase activity in other tissues. This probably explains why a greater efficacy, such as tumor stasis/regression, was not observed in this study.

The results presented here, as well as in our previous studies, reaffirmed our hypothesis that phospho-NSAIDs are a class of pharmacologically disparate identities from the NSAIDs from which they are derived (8, 9,14, 23), and that carboxylesterase-mediated hydrolysis leads to their inactivation. In this regard, phospho-NSAIDs are distinct from conventional ester prodrugs, such as irinotecan (24–26), capecitabine (27–29) and LY2334737 (30), which are bioactivated upon cleavage with carboxylesterases. Interestingly, it has been shown that esterase-knockout in mice (*Est1^c/scid*) has an opposing effect on the anticancer efficacy of irinotecan, a prodrug of SN-38, compared to wild-type mice (31). On the contrary, *Ces1c*-knockout improves the efficacy of phospho-NSAIDs. Hence, it is apparent that phospho-NSAIDs do not fulfil the definition of prodrugs, which presumably are devoid of biological activity. Mechanism(s) underlying the enhanced efficacy of phospho-NSAIDs are a subject of our on-going investigation. Whilst conventional NSAIDs are thought to suppress carcinogenesis in part via the inhibition of cyclooxygenase-2 (32), chemical modification with the phospho-moiety abrogates their ability to inhibit this enzyme (8). Several COX-independent molecular targets of phospho-NSAIDs have emerged in recent studies, such as the epidermal growth factor receptor (23), the thioredoxin system (11), and NF-KB (33).

Conclusion

In conclusion, our data indicate that the integrity of phospho-NSAIDs is critical for their anticancer activity, and that *Ces1c* $-/-$ mice are an appropriate model for preclinical evaluation of this class of drugs and others possessing a carboxylic ester moiety.

Supplementary Material

Refer to Web version on PubMed Central for supplementary material.

Acknowledgements

This work was supported by the National Institutes of Health (NIH) National Cancer Institute (NCI): Grant 5R01CA154172 and the Department of Defense (DOD): Grant W81XWH 11-1-0799.

Abbreviations

Ces1c	mouse plasma carboxylesterase isoform 1c
CES2	carboxylesterase 2
COX	cyclooxygenase
KPC	pancreatic carcinoma
LLC	Lewis lung carcinoma
NSAID	non-steroidal anti-inflammatory drug

PLA-PEG	polylactic acid-polyethylene glycol
P-S	phospho-sulindac
P-V	phospho-valproic acid

References

1. Clevers H. Colon cancer--understanding how NSAIDs work. *New Eng J Med.* 2006; 354:761–763. [PubMed: 16481647]
2. Scherubl H, Sutter AP, Zeitz M. NSAIDs and esophageal cancer. *Gastroenterology.* 2003; 125:1914–1915. author reply 5. [PubMed: 14727630]
3. Warner TD, Giuliano F, Vojnovic I, Bukasa A, Mitchell JA, Vane JR. Nonsteroid drug selectivities for cyclo-oxygenase-1 rather than cyclo-oxygenase-2 are associated with human gastrointestinal toxicity: a full in vitro analysis. *Proc Natl Acad Sci U S A.* 1999; 96:7563–7568. [PubMed: 10377455]
4. Graham DJ. COX-2 inhibitors, other NSAIDs, and cardiovascular risk - The seduction of common sense. *Jama-J Am Med Assoc.* 2006; 296:1653–1656.
5. Cuzick J, Otto F, Baron JA, Brown PH, Burn J, Greenwald P, et al. Aspirin and non-steroidal anti-inflammatory drugs for cancer prevention: an international consensus statement. *Lancet Oncol.* 2009; 10:501–507. [PubMed: 19410194]
6. Nie T, Wong CC, Alston N, Aro P, Constantinides PP, Rigas B. Phospho-ibuprofen (MDC-917) incorporated in nanocarriers: Anti-cancer activity in vitro and in vivo. *Brit J Pharmacol.* 2012; 166:991–1001. [PubMed: 22141583]
7. Huang L, Zhu C, Sun Y, Xie G, Mackenzie GG, Qiao G, et al. Phospho-sulindac (OXT-922) inhibits the growth of human colon cancer cell lines: a redox/polyamine-dependent effect. *Carcinogenesis.* 2010; 31:1982–1990. [PubMed: 20627873]
8. Mackenzie GG, Sun Y, Huang L, Xie G, Ouyang N, Gupta RC, et al. Phospho-sulindac (OXT-328), a novel sulindac derivative, is safe and effective in colon cancer prevention in mice. *Gastroenterology.* 2010; 139:1320–1332. [PubMed: 20600034]
9. Huang L, Mackenzie GG, Sun Y, Ouyang N, Xie G, Vrankova K, et al. Chemotherapeutic properties of phospho-nonsteroidal anti-inflammatory drugs, a new class of anticancer compounds. *Cancer Res.* 2011; 71:7617–7627. [PubMed: 22025561]
10. Zhu C, Cheng KW, Ouyang N, Huang L, Sun Y, Constantinides PP, et al. Phosphosulindac (OXT-328) Selectively Targets Breast Cancer Stem Cells In vitro and in Human Breast Cancer Xenografts. *Stem Cells.* 2012; 30:2065–2075. [PubMed: 22653497]
11. Sun Y, Rowehl LM, Huang L, Mackenzie GG, Vrankova K, Komninou D, et al. Phospho-ibuprofen (MDC-917) suppresses breast cancer growth: an effect controlled by the thioredoxin system. *Breast Cancer Res.* 2012; 14:R20. [PubMed: 22293394]
12. Zhu R, Cheng KW, Mackenzie G, Huang L, Sun Y, Xie G, et al. Phospho-Sulindac (OXT-328) Inhibits the Growth of Human Lung Cancer Xenografts in Mice: Enhanced Efficacy and Mitochondria Targeting by its Formulation in Solid Lipid Nanoparticles. *Pharm Res.* 2012; 29:3090–3101. [PubMed: 22723123]
13. Cheng KW, Mattheolabakis G, Wong CC, Ouyang N, Huang L, Constantinides PP, et al. Topical phospho-sulindac (OXT-328) is effective in the treatment of non-melanoma skin cancer. *Int J Oncol.* 2012; 41:1199–1203. [PubMed: 22842609]
14. Satoh T, Hosokawa M. The mammalian carboxylesterases: from molecules to functions. *Annu. Rev. Pharmacol. Toxicol.* 1998; 38:257–288. [PubMed: 9597156]
15. Marsha S, Xiao M, Yu J, Ahluwalia R, Minton M, Freimuth RR, et al. Pharmacogenomic assessment of carboxylesterases 1 and 2. *Genomics.* 2004; 84:661–668. [PubMed: 15475243]
16. Wong CC, Cheng KW, Xie G, Zhou D, Zhu CH, Constantinides PP, et al. Carboxylesterases 1 and 2 hydrolyze phospho-nonsteroidal anti-inflammatory drugs: relevance to their pharmacological activity. *J Pharmacol Exp Ther.* 2012; 340:422–432. [PubMed: 22085648]

17. Xie G, Nie T, Mackenzie GG, Sun Y, Huang L, Ouyang N, et al. The metabolism and pharmacokinetics of phospho-sulindac (OXT-328) and the effect of difluoromethylornithine. *Brit J Pharmacol.* 2012; 165:2152–2166. [PubMed: 21955327]
18. Xie G, Sun Y, Nie T, Mackenzie GG, Huang L, Kopelovich L, et al. Phospho-ibuprofen (MDC-917) is a novel agent against colon cancer: efficacy, metabolism, and pharmacokinetics in mouse models. *J Pharmacol Exp Ther.* 2011; 337:876–886. [PubMed: 21422165]
19. Li B, Sedlacek M, Manoharan I, Boopathy R, Duysen EG, Masson P, et al. Butyrylcholinesterase, paraoxonase, and albumin esterase, but not carboxylesterase, are present in human plasma. *Biochem Pharmacol.* 2005; 70:1673–1684. [PubMed: 16213467]
20. Duysen EG, Koentgen F, Williams GR, Timperley CM, Schopfer LM, Cerasoli DM, et al. Production of ES1 plasma carboxylesterase knockout mice for toxicity studies. *Chem Res Toxicol.* 2011; 24:1891–1898. [PubMed: 21875074]
21. Zhang Y, Huo M, Zhou J, Xie S. PKSolver: An add-in program for pharmacokinetic and pharmacodynamic data analysis in Microsoft Excel. *Comput Methods Programs Biomed.* 2010; 99:306–314. [PubMed: 20176408]
22. Mackenzie GG, Huang L, Alston N, Ouyang N, Vrankova K, Mattheolabakis G, et al. Targeting mitochondrial STAT3 with the novel phospho-valproic acid (MDC-1112) inhibits pancreatic cancer growth in mice. *PLoS one.* 2013; 8:e61532. [PubMed: 23650499]
23. Cheng KW, Wong CC, Alston N, Mackenzie GG, Huang L, Ouyang N, et al. Aerosol administration of phospho-sulindac inhibits lung tumorigenesis. *Mol Cancer Ther.* 2013; 12:1417–1428. [PubMed: 23645590]
24. Khanna R, Morton CL, Danks MK, Potter PM. Proficient metabolism of irinotecan by a human intestinal carboxylesterase. *Cancer Res.* 2000; 60:472–478.
25. Humerickhouse R, Lohrbach K, Li L, Bosron WF, Dolan ME. Characterization of CPT-11 hydrolysis by human liver carboxylesterase isoforms hCE-1 and hCE-2. *Cancer Res.* 2000; 60:1189–1192. [PubMed: 10728672]
26. Guichard SM, Morton CL, Krull EJ, Stewart CF, Danks MK, Potter PM. Conversion of the CPT-11 metabolite APC to SN-38 by rabbit liver carboxylesterase. *Clin Cancer Res.* 1998; 4:3089–3094. [PubMed: 9865925]
27. Quinney SK, Sanghani SP, Davis WI, Hurley TD, Sun Z, Murry DJ, et al. Hydrolysis of capecitabine to 5'-deoxy-5-fluorocytidine by human carboxylesterases and inhibition by loperamide. *J Pharmacol Exp Ther.* 2005; 313:1011–1016. [PubMed: 15687373]
28. Tabata T, Katoh M, Tokudome S, Nakajima M, Yokoi T. Identification of the cytosolic carboxylesterase catalyzing the 5'-deoxy-5-fluorocytidine formation from capecitabine in human liver. *Drug Metab Dispos.* 2004; 32:1103–1110. [PubMed: 15269188]
29. Miwa M, Ura M, Nishida M, Sawada N, Ishikawa T, Mori K, et al. Design of a novel oral fluoropyrimidine carbamate, capecitabine, which generates 5-fluorouracil selectively in tumours by enzymes concentrated in human liver and cancer tissue. *Eur J Cancer.* 1998; 34:1274–1281. [PubMed: 9849491]
30. Pratt SE, Durland-Busbice S, Shepard RL, Heinz-Taheny K, Iversen PW, Dantzig AH. Human carboxylesterase-2 hydrolyzes the prodrug of gemcitabine (LY2334737) and confers prodrug sensitivity to cancer cells. *Clin Cancer Res.* 2013; 19:1159–1168. [PubMed: 23325581]
31. Morton CL, Iacono L, Hyatt JL, Taylor KR, Cheshire PJ, Houghton PJ, et al. Activation and antitumor activity of CPT-11 in plasma esterase-deficient mice. *Cancer Chemoth Pharm.* 2005; 56:629–636.
32. Kurumbail RG, Stevens AM, Gierse JK, McDonald JJ, Stegeman RA, Pak JY, et al. Structural basis for selective inhibition of cyclooxygenase-2 by anti-inflammatory agents. *Nature.* 1996; 384:644–648. [PubMed: 8967954]
33. Zhou D, Papayannis I, Mackenzie GG, Alston N, Ouyang N, Huang L, et al. The anticancer effect of phospho-tyrosol-indomethacin (MPI-621), a novel phosphoderivative of indomethacin: in vitro and in vivo studies. *Carcinogenesis.* 2012; 34:943–951. [PubMed: 23338686]

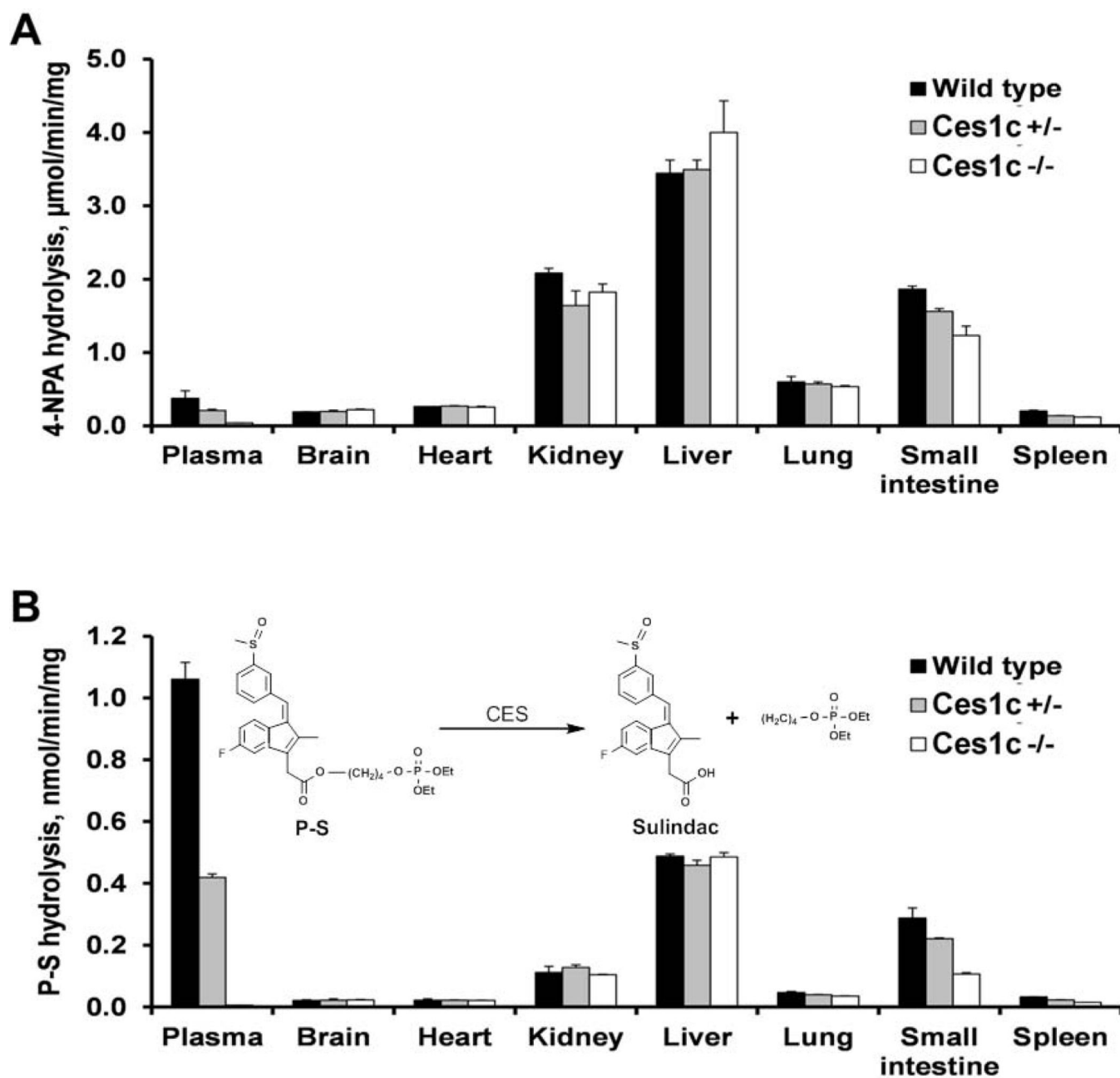


Figure 1. Carboxylesterase activity in the blood and organs of wild-type, *Ces1c* +/- and *Ces1c* -/- mice

The plasma and organs were incubated with (A) 1 mM 4-nitrophenyl acetate (4-NPA) (incubation time: 2min) or (B) 100 μ M phospho-sulindac (P-S) (incubation time: 1h) in phosphate-buffered saline at 37°C, and the rate of hydrolysis was measured by spectrophotometry or HPLC.

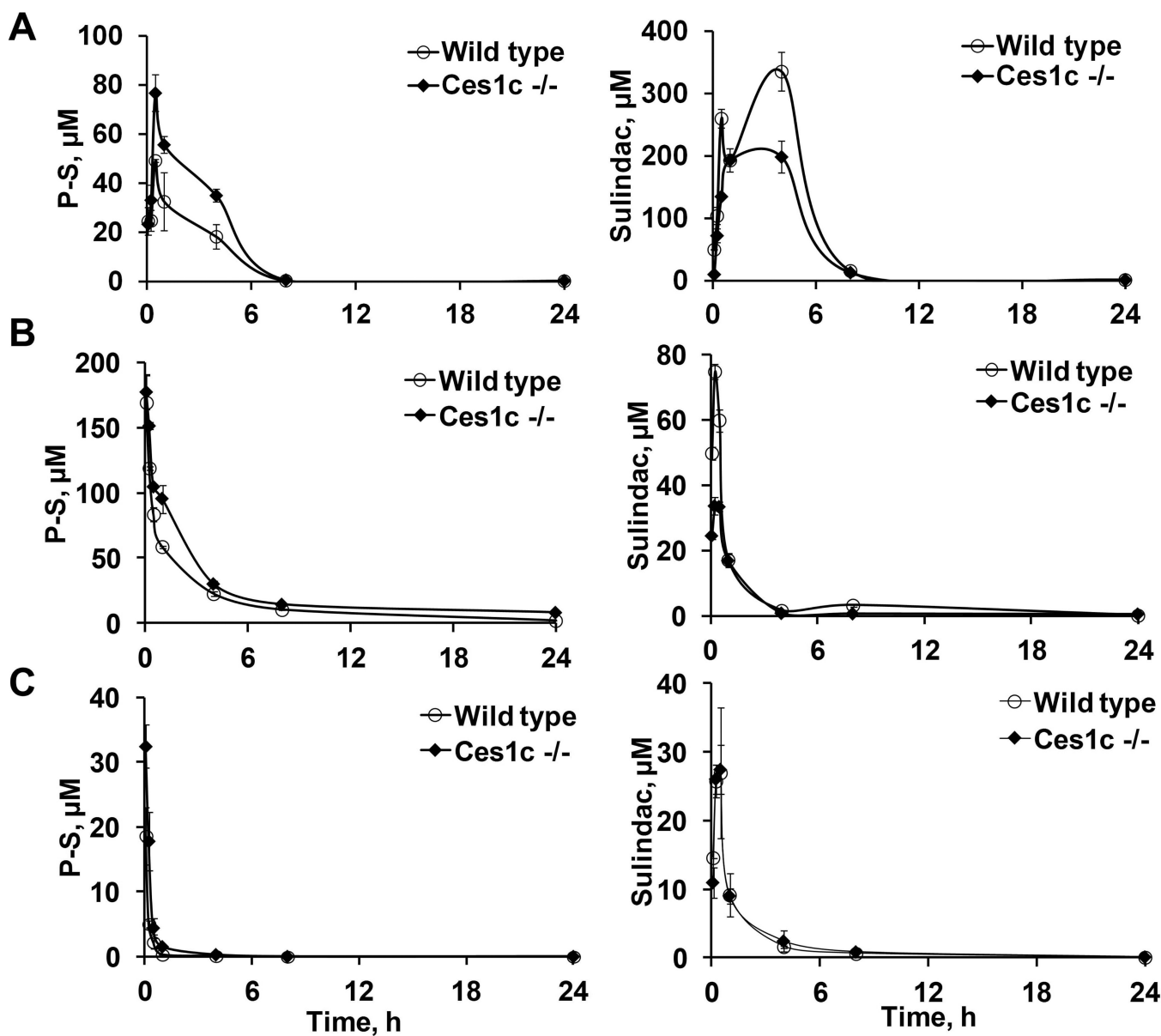


Figure 2. Pharmacokinetic studies of phospho-sulindac in wild-type and *Ces1c* $-/-$ mice
 Blood levels of phospho-sulindac (P-S) and sulindac in wild-type and *Ces1c* $-/-$ mice after a single dose of (A) P-S (300mg/kg i.p.), (B) PLA-PEG P-S (50mg/kg, i.v.) and (C) Pluronic P123 P-S (50mg/kg, i.v.), respectively.

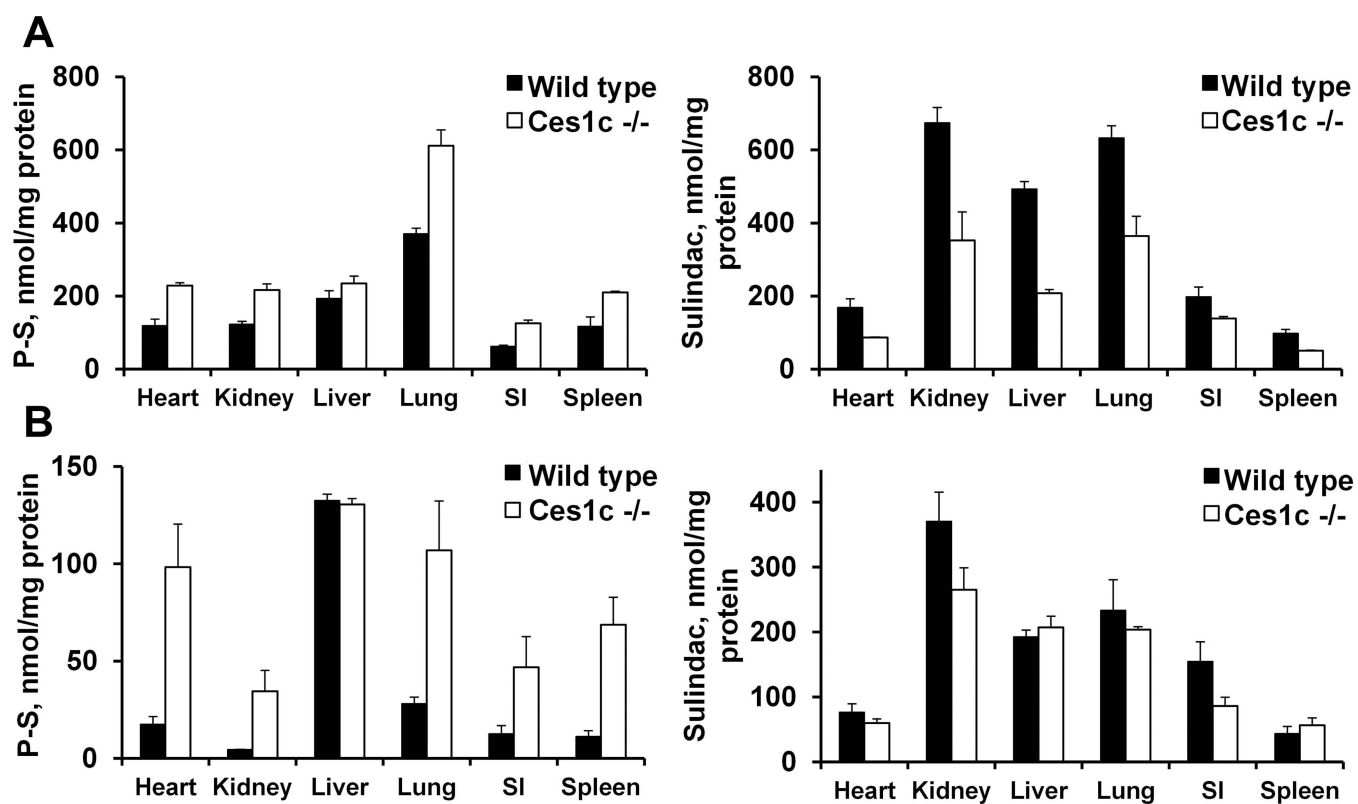


Figure 3. Biodistribution of phospho-sulindac in wild-type and *Ces1c* $-/-$ mice. Tissue levels of phospho-sulindac (P-S) and sulindac in wild-type and *Ces1c* $-/-$ mice after a single dose of (A) PLA-PEG P-S (50mg/kg, i.v.) and (B) Pluronic P-S (50mg/kg, i.v.), respectively.

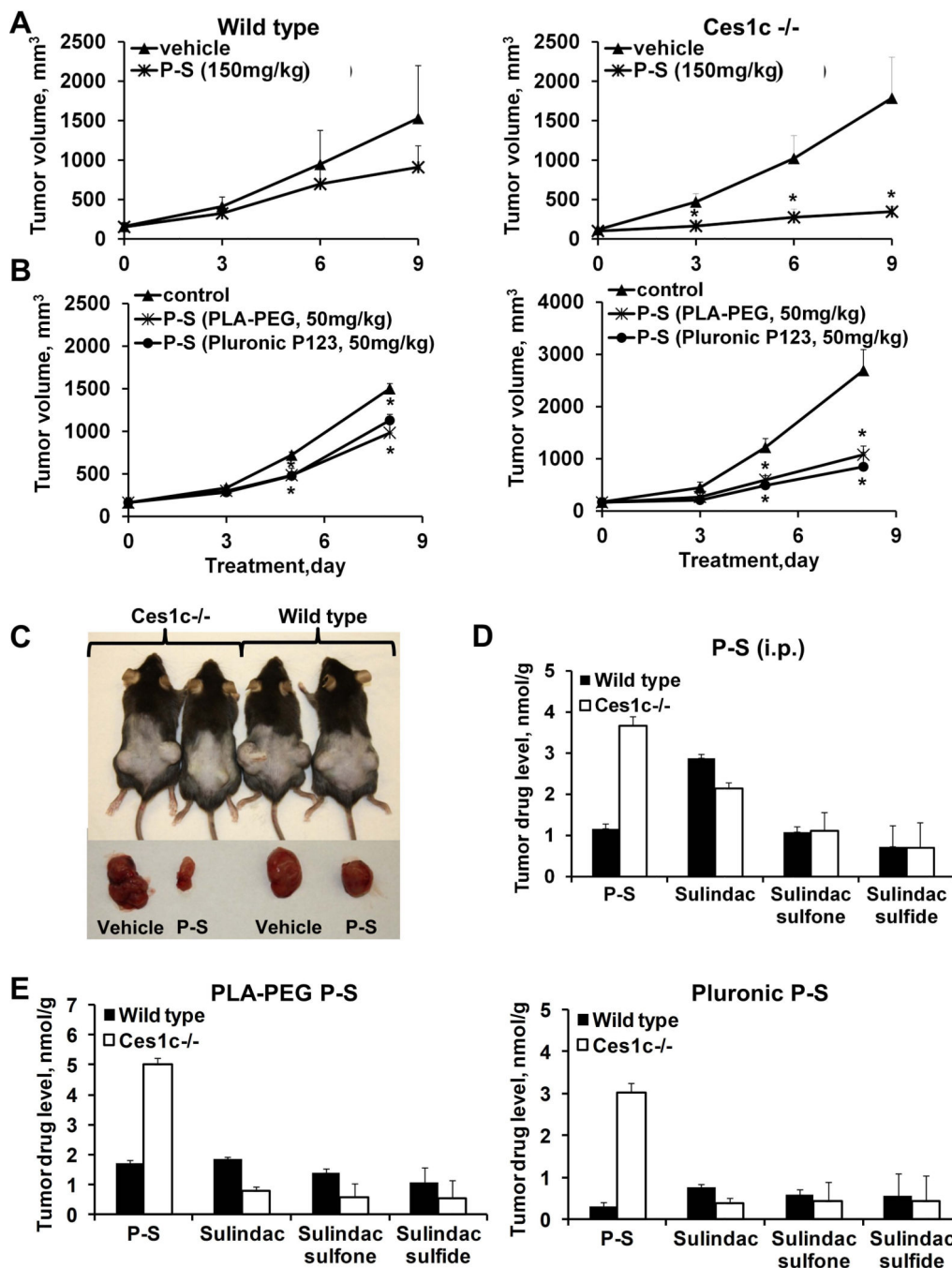


Figure 4. P-S is more efficacious against lewis lung carcinoma (LLC) in Ces^{-/-} mice
 (A) Efficacy of P-S (150mg/kg, i.p.) in wild-type (left) and Ces1c^{-/-} mice (right) bearing subcutaneous LLC tumors. (B) Efficacy of PLA-PEG P-S (50mg/kg, i.v.) and Pluronic P123 P-S (50mg/kg, i.v.) in wild-type (left) and Ces1c^{-/-} (right) mice bearing subcutaneous tumors. (C) Representative images (left) of the mice and tumors treated with vehicle or P-S (150mg/kg, i.p.), tumor drug levels at end point (right). (D) Tumor drug levels of mice treated with PLA-PEG P-S (left) and Pluronic P123 (right). *, *p*<0.05.

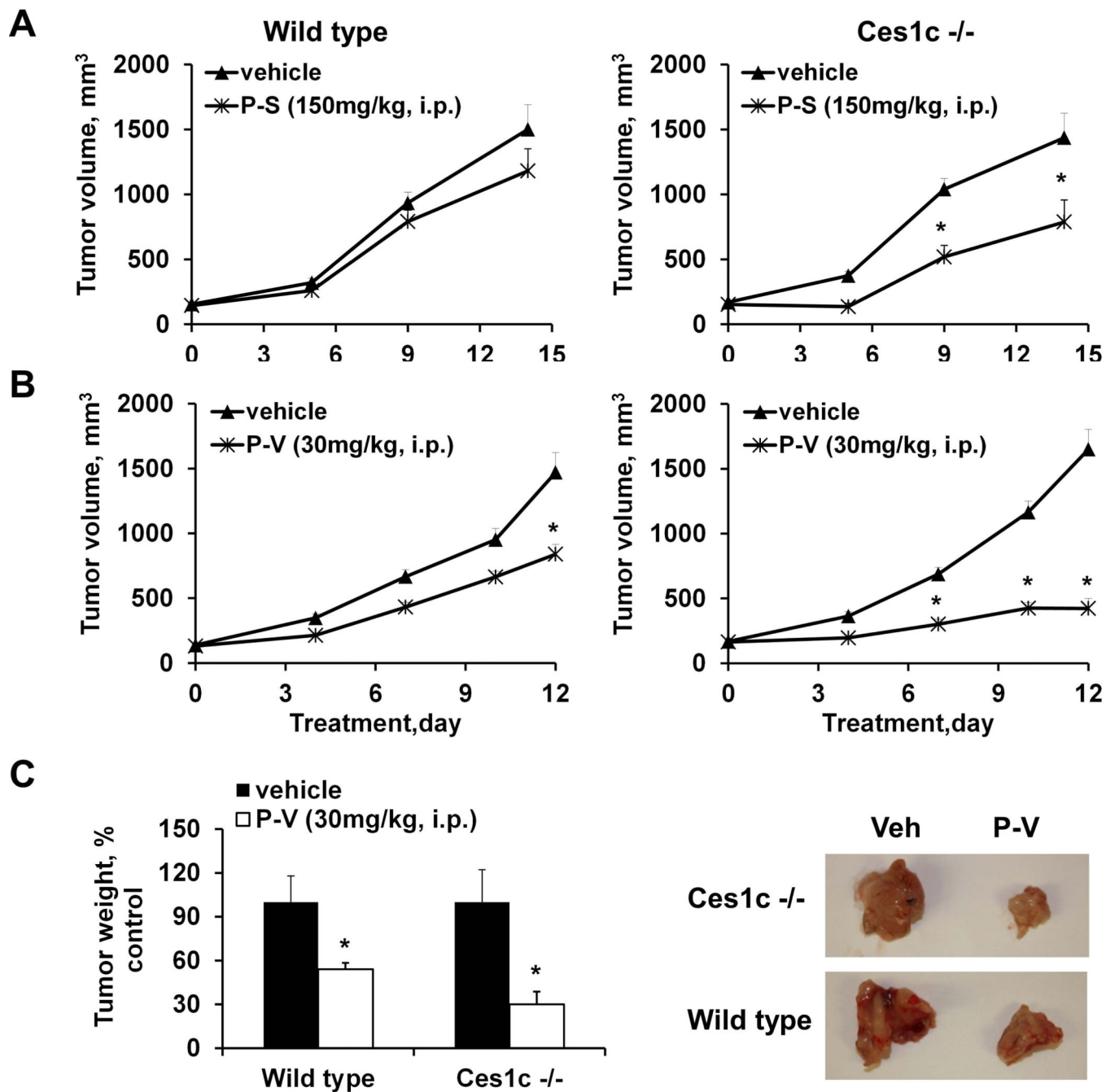


Figure 5. P-S and P-V are more efficacious against pancreatic carcinoma (KPC) in Ces^{-/-} mice
 (A) Efficacy of P-S (150mg/kg, i.p.) in wild-type (left) and Ces1c^{-/-} mice (right) bearing subcutaneous KPC tumors. (B) Efficacy of P-V (30mg/kg, i.p.) in wild-type (left) and Ces1c^{-/-} (right) mice bearing subcutaneous KPC tumors. (C) Efficacy of P-V (30mg/kg, i.p.) in wild-type and Ces1c^{-/-} mice bearing orthotopic KPC tumors (left); and representative images (right) of the orthotopic KPC tumors from vehicle and P-S (150mg/kg, i.p.) treatment groups. *, $p < 0.05$.

Table 1

Kinetics of phospho-NSAID hydrolysis by murine plasma carboxylesterase expressed in 293T cell lysates.

	K_m , μM	V_{max} nmol/min/mg*
Phospho-aspirin (MDC-46)	138	2.5
Phospho-aspirin (MDC-22)	270	4.0
Phospho-ibuprofen	34.9	10.7
Phospho-indomethacin	25.1	2.2
Phospho-tyrosol-indomethacin	16.6	55.8
Phospho-naproxen	48.1	34.4
Phospho-sulindac	92.5	0.7

* Protein concentration was determined by the Bradford assay.

Table 2

Plasma carboxylesterase activity in wild-type, *Ces1c* +/-, *Ces1c* -/- mice and human plasma. Hydrolytic activity was measured at 100µM substrate concentration.

	Species	Genotype	Hydrolytic activity, nmol/min/mg	Activity, relative to human
Phospho-aspirin (MDC-46)	Mouse	Wild-type	1.87 ± 0.37	5.8
		<i>Ces1c</i> +/-	1.48 ± 0.07	4.6
		<i>Ces1c</i> -/-	0.33 ± 0.02	1.0
	Human		0.32 ± 0.00	
Phospho-aspirin (MDC-22)	Mouse	Wild-type	5.47 ± 0.22	270
		<i>Ces1c</i> +/-	4.24 ± 0.98	210
		<i>Ces1c</i> -/-	2.81 ± 0.18	140
	Human		0.02 ± 0.00	
Phospho-ibuprofen	Mouse	Wild-type	1.77 ± 0.44	25
		<i>Ces1c</i> +/-	1.13 ± 0.04	16
		<i>Ces1c</i> -/-	0.33 ± 0.03	4.7
	Human		0.07 ± 0.01	
Phospho-indomethacin	Mouse	Wild-type	0.45 ± 0.15	11
		<i>Ces1c</i> +/-	0.22 ± 0.03	5.5
		<i>Ces1c</i> -/-	0.02 ± 0.00	0.5
	Human		0.04 ± 0.00	
Phospho-tyrosol-indomethacin	Mouse	Wild-type	2.30 ± 0.01	25
		<i>Ces1c</i> +/-	2.29 ± 0.05	25
		<i>Ces1c</i> -/-	0.32 ± 0.01	3.6
	Human		0.09 ± 0.01	
Phospho-naproxen	Mouse	Wild-type	5.68 ± 1.66	19
		<i>Ces1c</i> +/-	3.10 ± 0.19	10
		<i>Ces1c</i> -/-	0.49 ± 0.00	1.6
	Human	n.d.	0.30 ± 0.02	
Phospho-sulindac	Mouse	Wild-type	1.06 ± 0.05	530
		<i>Ces1c</i> +/-	0.42 ± 0.01	210
		<i>Ces1c</i> -/-	0.01 ± 0.00	5.0
	Human		0.002 ± 0.001	

Table 3

Effect of *Ces1c* expression on the cytotoxicity of phospho-NSAIDs. The *Ces1c*/Control ratios represent the fold changes in IC₅₀ in 293T-*Ces1c* cells as compared to 293T-Control cells.

	IC ₅₀ , μ M		<i>Ces1c</i> / Control ratio
	293T- Control	293T- <i>Ces1c</i>	
Phospho-aspirin (MDC-46)	953 \pm 34	787 \pm 26	0.8
Phospho-aspirin (MDC-22)	507 \pm 14	755 \pm 197	1.5
Phospho-ibuprofen	62 \pm 6	775 \pm 96	13
Phospho-indomethacin	45 \pm 1	101 \pm 3	2.3
Phospho-tyrosol-indomethacin	59 \pm 3	297 \pm 27	5.0
Phospho-naproxen	69 \pm 5	1280 \pm 370	19
Phospho-sulindac	28 \pm 2	112 \pm 7	4.0
Phospho-valproic acid	41 \pm 2	105 \pm 16	2.6

Effect of wild-type (WT) and *Ces1c* $-/-$ mouse serum (5%) on the cytotoxicity of phospho-NSAIDs. The cytotoxicity (24h- IC_{50} values, μ M) of phospho-NSAIDs was determined by the MTT assay.

Table 4

	Lewis Lung Carcinoma (LLC)			Pancreatic Carcinoma (KPC)		
	FBS	WT serum	<i>Ces1c</i> $-/-$ serum	FBS	WT serum	<i>Ces1c</i> $-/-$ serum
Phospho-aspirin (MDC-46)	$> 2,000$	$> 2,000$	$> 2,000$	$> 2,000$	$> 2,000$	$< 2,000$
Phospho-aspirin (MDC-22)	755 ± 23	1170 ± 20	1080 ± 28	848 ± 53	1820 ± 70	1080 ± 30
Phospho-ibuprofen	65 ± 4	395 ± 23	140 ± 2	72 ± 2	513 ± 11	76 ± 5
Phospho-indomethacin	67 ± 1	891 ± 25	61 ± 2	82 ± 3	643 ± 24	98 ± 2
Phospho-tyrosol-indomethacin	138 ± 38	$> 2,000$	175 ± 56	$> 2,000$	$> 2,000$	$> 2,000$
Phospho-naproxen	266 ± 9	$> 2,000$	441 ± 52	498 ± 15	$> 2,000$	780 ± 32
Phospho-sulindac	68 ± 1	465 ± 17	69 ± 1	66 ± 4	800 ± 119	76 ± 11
Phospho-valproic acid	63 ± 14	$> 2,000$	128 ± 4	29 ± 3	$> 2,000$	82 ± 2

Table 5

Pharmacokinetic parameters for P-S.

Pharmacokinetic parameters	P-S (300 mg/kg, i.p.)		PLA-PEG P-S (50 mg/kg, i.v.)		Pluronic P123 P-S (40mg/kg, i.v.)	
	Wild type	Ces1c -/-	Wild type	Ces1c -/-	Wild type	Ces1c -/-
C_0 , μM	-	-	178	173	33.8	46.0
C_{max} , μM	40.4	76.8	169	177	19.0	32.1
T_{max} , h	0.55	1.25	0.08	0.08	0.08	0.08
$\text{AUC}_{0-24\text{h}}$, $\mu\text{M}\cdot\text{h}$	155	261	136	284	4.69	11.3
$t_{1/2}$, h	2.24	0.87	0.53	1.14	0.09	0.17
CL, mg/ $\mu\text{M}/\text{h}$	0.04	0.02	0.007	0.004	0.17	0.07
V_{ss} , mg/ μM	-	-	0.006	0.006	0.02	0.02